Liquefaction evaluation for an interbedded soil deposit: St. Teresa's School, Christchurch, New Zealand

Ross W. Boulanger[1], F. ASCE, Mohammad Khosravi[2], M. ASCE,
Brady R. Cox[3], M. ASCE, and Jason T. DeJong[1], M. ASCE

[1]Professor, University of California, Davis, CA 95616
[2]Post-doctoral Researcher, University of California, Davis, CA 95616
[3]Professor, University of Texas, Austin, TX

ABSTRACT: Liquefaction vulnerability indices (LVIs) are computed for an interbedded soil site at St. Teresa's School, Christchurch, New Zealand to evaluate how various factors may have contributed to the standard LVI computations overestimating the potential for liquefaction damages during the 2010-2011 Canterbury Earthquake Sequence. The observed performance of the St. Teresa School site and its subsurface conditions are reviewed. An inverse filtering procedure is used to correct the cone penetration test (CPT) data for thin-layer and transition zone effects. LVI indices are computed using the CPT data from the site for a range of assumptions, including common default practices, site-specific fines content calibrations, inverse filtering of the CPT data, uncertainty in the triggering correlation, uncertainties in the correlations for shear and volumetric strains, and partial saturation. Other sources of potential conservatism in the LVI evaluations are discussed, including the potential contributions of the surface crust layer, dynamic response and excess pore water pressure diffusion.

INTRODUCTION

Case history studies have shown that liquefaction evaluations using various one-dimensional (1-D) liquefaction vulnerability indices (LVIs) tend to over-predict the potential for earthquake-induced liquefaction effects in interbedded deposits of sand, silt and clay. One-dimensional LVIs are computed using data from individual borings or cone penetration test (CPT) soundings, and include the lateral displacement index (LDI), liquefaction potential index (LPI), liquefaction severity number (LSN), and post-liquefaction reconsolidation settlement ($S_{v\text{-}1D}$). The tendency for LVIs, computed following common practices, to over-predict liquefaction effects at interbedded sites was observed for several areas of Christchurch, New Zealand, during the 2010-2011 Canterbury Earthquake Sequence (e.g., Beyzaei et al. 2018, Maurer et al. 2014, Stringer et al. 2015, van Ballegooy et al. 2014, 2015).

The potential for standard LVIs or other liquefaction analysis procedures to over-

predict liquefaction effects in interbedded deposits of sand, silt, and clay may be attributed to several factors, each of which may be important in different situations or for different analysis procedures. Possible factors can be grouped into those associated with (Boulanger et al. 2016): (1) limitations in site characterization tools and procedures, (2) limitations in liquefaction triggering or consequence correlations, and (3) limitations in the analysis procedures and the role of neglected mechanisms. The first group of limitations includes challenges with characterizing thin layers, transition zones, graded beddings, lateral continuity of lenses, and partial saturation below the groundwater table. The second group of limitations includes uncertainty in the correlations for cyclic resistance ratio (CRR), shear strain potential, or post-liquefaction reconsolidation strain, given they are generally not well-constrained for intermediate soils (e.g., low-plasticity silty sands, sandy silts, and silts) and do not explicitly account for factors such as age, stress-strain history, over-consolidation, or cementation. The third group of limitations includes challenges with accounting for spatial variability, the beneficial effect of thick crust layers, key features of the nonlinear dynamic response, the two- or three-dimensional geometry of any deformation mechanism, and the role of excess pore pressure diffusion. For interbedded sites where LVIs have over-predicted the effects of liquefaction in past earthquakes, the bias toward over-prediction is likely due to the cumulative effects of several of these limitations.

An inverse filtering procedure was recently developed by Boulanger and DeJong (2018) to provide an objective, repeatable, and automatable means for correcting CPT data for thin layer and transition zone effects, with a specific focus on eventual application to liquefaction evaluation problems. The inverse filtering procedure has three primary components: (1) a model for how the cone penetrometer acts as a low-pass spatial filter in sampling the true distribution of soil resistance versus depth, (2) a solution procedure for iteratively determining an estimate of the true cone penetration resistance profile from the measured profile given the cone penetration filter model, and (3) a procedure for identifying sharp transition interfaces and correcting the data at those interfaces. The inverse filtering procedure was developed to improve the interpretation of CPT data in interbedded deposits, while recognizing that any inversion process will be neither unique nor perfect.

The present study examines the application of LVI procedures to the interbedded soil site at St. Teresa's School in Christchurch, New Zealand to evaluate how certain assumptions and factors may have contributed to the standard LVI computations over-estimating the potential for liquefaction damages during the 2010-2011 Canterbury Earthquake Sequence. The observed performance of the site and its subsurface conditions are described, followed by a brief summary of the inverse filtering procedure that is used to correct the CPT data for thin-layer and transition zone effects. LVI indices are computed using the CPT data with a range of assumptions to evaluate alternate practices and key sources of uncertainty. LVI results are presented for cases that consider common industry standard practices, site-specific fines content calibrations, inverse filtering of the CPT data, uncertainty in the triggering correlation, uncertainties in the correlations for shear and volumetric strains, and partial saturation. Other sources of potential conservatism in the LVI-based liquefaction evaluations are discussed, including the potential roles of the

surface crust layer, dynamic response, and pore pressure diffusion. The implications of these results for practice and future research needs are addressed.

ST. TERESA'S SCHOOL: SITE DATA

St. Teresa's School, located in the Riccarton suburb of Christchurch, New Zealand, had no observed manifestation of liquefaction during the September 2010 M_w=7.1 Darfield earthquake or the February 2011 M_w=6.2 Christchurch earthquake. The peak ground acceleration (PGA) at the site was estimated to be about 0.22 g and 0.34 g for these two earthquakes, respectively (Cox et al. 2017), based on the conditional distributions described in Green et al. (2014) and Bradley (2014). The buildings at the site were single story structures on shallow foundations.

The aerial view in Figure 1 indicates the locations of the four CPT soundings, two borings, and direct-push cross-hole (DPCH) tests performed at the site. The CPT and borehole data were obtained from the New Zealand Geotechnical Database (NZGD 2018) and the DPCH data were previously described in Cox et al. (2017).

The cross-sectional profile in Figure 2 shows the borehole and CPT data along the north-south section labeled on Figure 1. The cone tip resistances ($q_{tN} = q_t/P_a$, where P_a = atmospheric pressure) are colored coded by the Soil Behavior Type Index (I_c) ranges that approximately separate silt mixtures ($I_c \geq 2.6$), sand mixtures ($2.05 \leq I_c < 2.6$), and sands ($I_c < 2.05$) (Robertson 1990, 2009). The surface layer of fill or reworked material appears to be less than about 1 m thick, and is underlain by a stratum of interbedded silt, sandy silt, silty sand and sand to a depth of about 17 m. The borehole data for this stratum (Figure 2) indicate that the silts have fines contents (FC) of 84-92% and plasticity indices (PI) of 4-8, the majority of the stratum is comprised of sandy silts and silty sands with FC of 44-59% (average 52%), and there are relatively few, thin lenses of clean sands. The stratum below 17 m is comprised of dense and very dense sand and gravel. The groundwater table is at a depth of about 1.1 m.

The compression wave velocity (V_p) and shear wave velocity (V_s) data from the DPCH testing (Figure 3) indicates that the soils are partially saturated to depths of about 5.5 m. The V_p ranges from 800-1,100 m/s for depths of 2.2-5.0 m, and then increases to about 1,600 m/s for depths of 5.5 m and greater.

Profiles of undrained shear strength ratio (s_u/σ'_{vc}) for the silts that classify as clay-like based on $I_c > 2.6$ were computed using a cone bearing factor (N_{kt}) of 14. The resulting profiles of s_u/σ'_{vc} for SCPT 57345 are shown in Figure 3 using both the measured CPT data and the inverse filtered CPT data (details of the inverse filtering are described later). The s_u/σ'_{vc} for the weaker intervals at depths of 15-17 m are in the range expected for normally consolidated clay-like soils (e.g., 0.22±). The s_u/σ'_{vc} ratios progressively increase with decreasing depth, with the lowest values reaching 0.4-0.6 near a depth of 5.5 m and 0.8-1.2 near a depth of 2 m. This profile of s_u/σ'_{vc} is consistent with the effect that a prior lower water table (e.g., perhaps to depths of 4-6 m) would have had on consolidation stress history throughout the profile. Prior water table fluctuations would also be consistent with the soils being partially saturated above depths of 5.5 m, as indicated by the low V_p values.

FIG. 1. Location of subsurface explorations at St. Teresa's School (base image sourced from the New Zealand Geotechnical Database 2018).

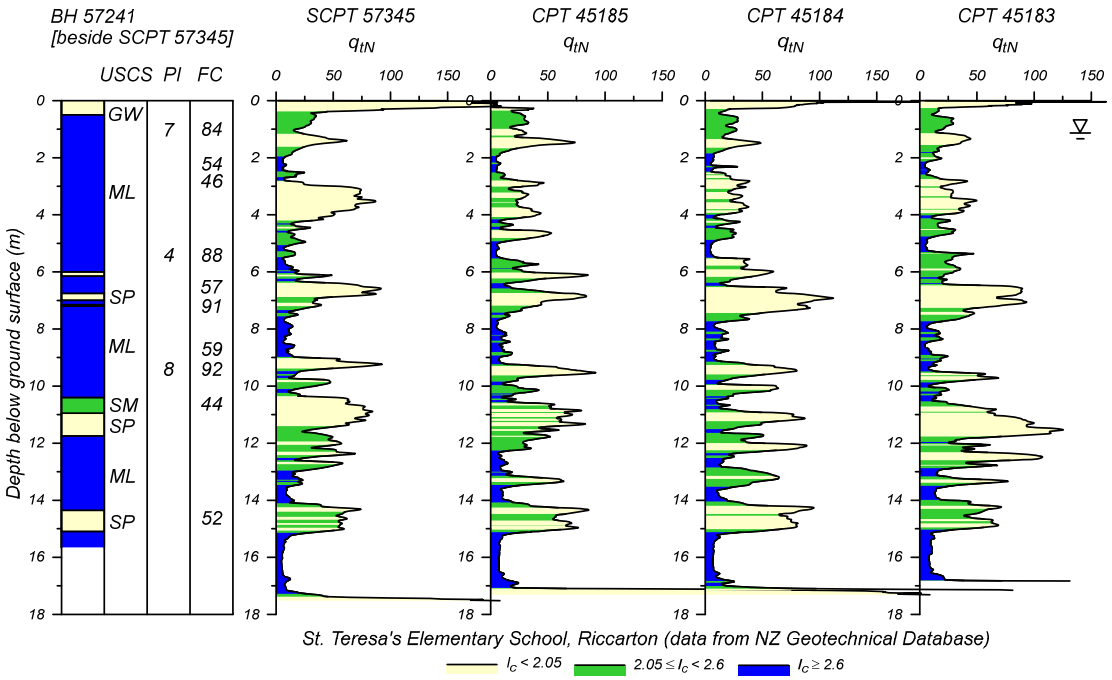

FIG. 2. North-south section across St. Teresa's School site.

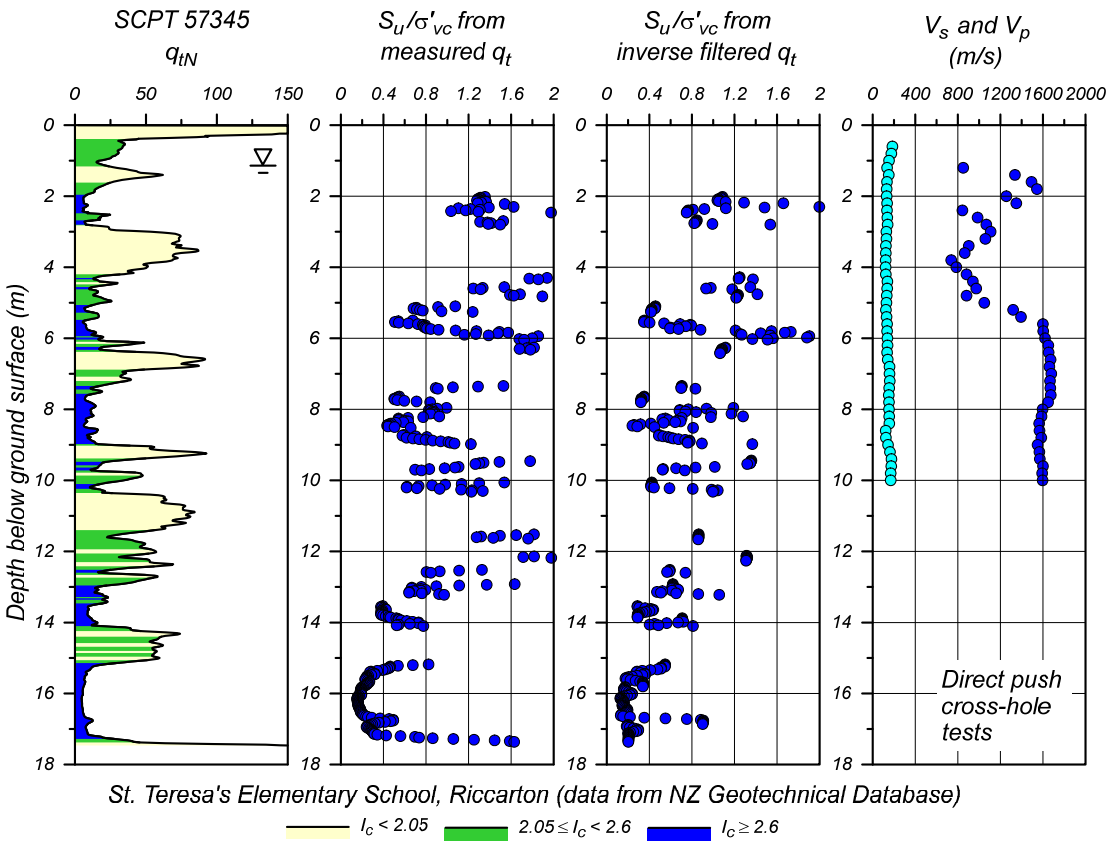

FIG. 3. SCPT 57345: (a) q_{tN} profile, (b) undrained shear strength ratios from measured CPT data, (c) undrained shear strength ratios from inverse filtered CPT data, and (d) V_s and V_p profiles from direct-push, cross-hole tests.

INVERSE FILTERING OF CPT DATA

An inverse filtering procedure was developed by Boulanger and DeJong (2018) to provide an objective, repeatable, and automatable means for correcting CPT data for thin layer and transition zone effects. The inverse filtering procedure has three primary components: (1) a model for how the cone penetrometer acts as a low-pass spatial filter in sampling the true distribution of soil resistance versus depth, (2) a solution procedure for iteratively determining an estimate of the true cone penetration resistance profile from the measured profile given the cone penetration filter model, and (3) a procedure for identifying sharp transition interfaces and correcting the data at those interfaces. Detailed descriptions of the inverse filtering procedure and its evaluation against experimental, numerical, and field data are provided in Boulanger and DeJong (2018).

One of the ways that the inverse filtering procedure was evaluated was by generating equivalent thin layer correction factors for the idealized case of a uniform strong layer (with a true tip resistance of q^t_{strong}) embedded in a uniform weak material (with a true tip resistance of q^t_{weak}). The thin layer correction factor is q^t_{strong} divided by the peak tip resistance measured in the stronger layer (q^m_{peak}). The

equivalent thin layer correction factors derived by Boulanger and DeJong (2018) using a baseline set of inverse filtering parameters are shown in Figure 4. These equivalent thin layer correction factors include dependence on the q^t_{strong}/q^t_{weak} ratio and were calibrated using data from experimental and numerical studies (e.g., Ahmadi and Robertson 2005, Xu and Lehane 2008, Mo et al. 2017, Khosravi et al. 2018). The baseline set of parameters used to generate Figure 4 were also used for the inverse filtering in the present study.

Profiles of q_{tN} and I_c for the measured and inverse filtered SCPT 57345 are shown in Figure 5. The inverse filtering results in increased q_{tN} values for the stronger thin layers and decreased q_{tN} in the weaker thin layers, as expected. The interface detection and correction scheme replaces many of the transition zones in the measured profile with discrete steps in q_{tN} values for the inverse filtered profile. The reduction in q_{tN} in the thin, weaker silt layers is why the inverse filtered data produced smaller undrained shear strength ratios for the clay-like soils (as shown previously in Figure 3).

The cross-sectional profile for the site with the inverse filtered CPT data is shown in Figure 6. Comparing the profiles in Figures 2 and 6, the inverse filtering generated an overall increase in the portion of the profile that the CPT data would classify as sand ($I_c < 2.05$), which is a direct consequence of increasing the q_{tN} (and thereby decreasing the I_c) in the numerous thin, stronger layers. The effects of inverse filtering on the estimated properties of the sand-like soils for the purpose of liquefaction evaluations is examined in greater detail in the next section.

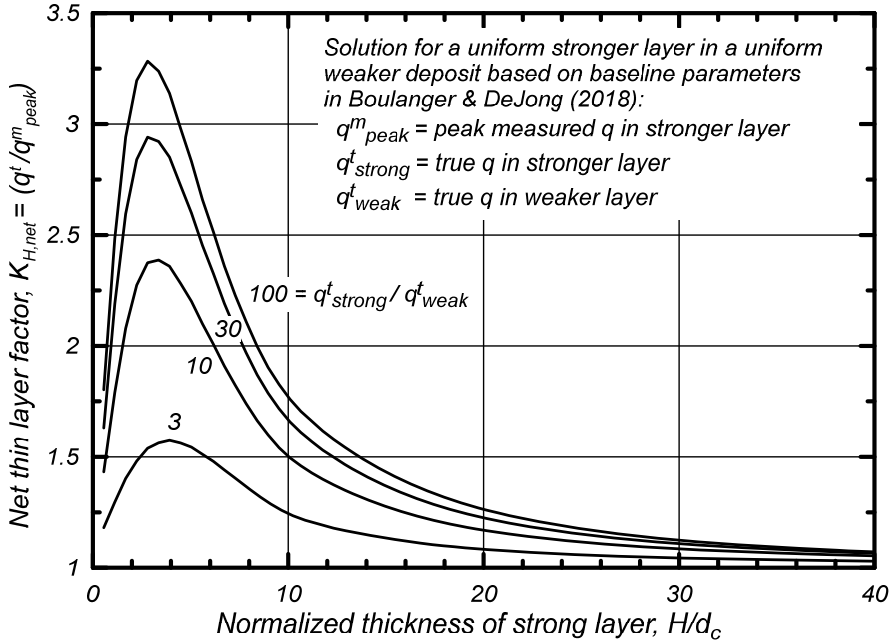

FIG. 4. Net thin-layer correction factor for a strong layer embedded in a weak deposit based on the inverse filtering procedure by Boulanger and DeJong (2018) with a baseline set of filter parameters.

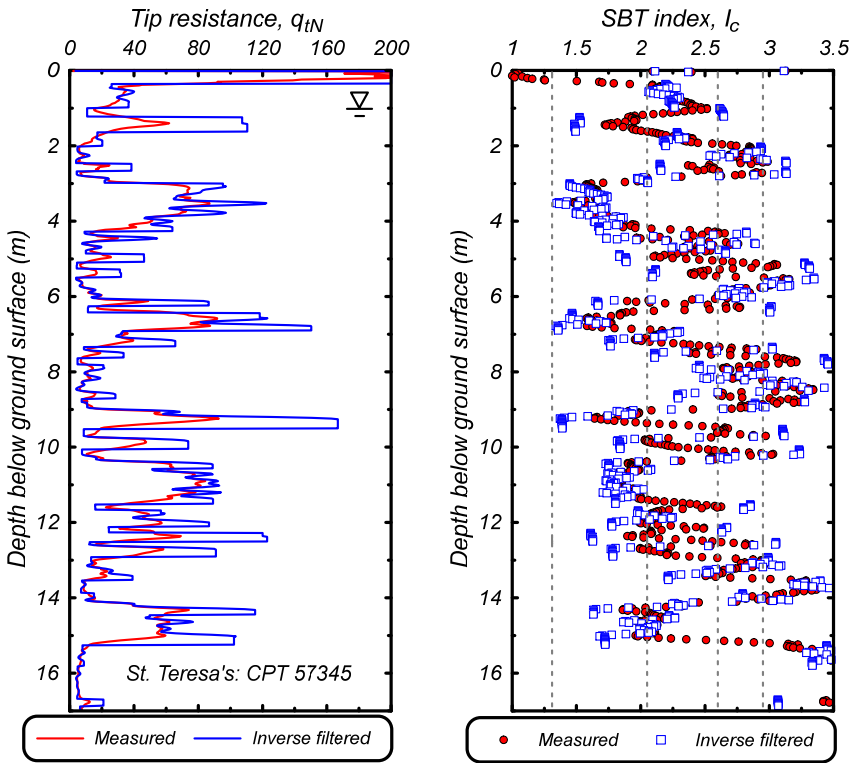

FIG. 5. Measured and inverse filtered profiles for (a) tip resistance q_{tN} and (b) Soil Behavior Type Index I_c for SCPT 57345.

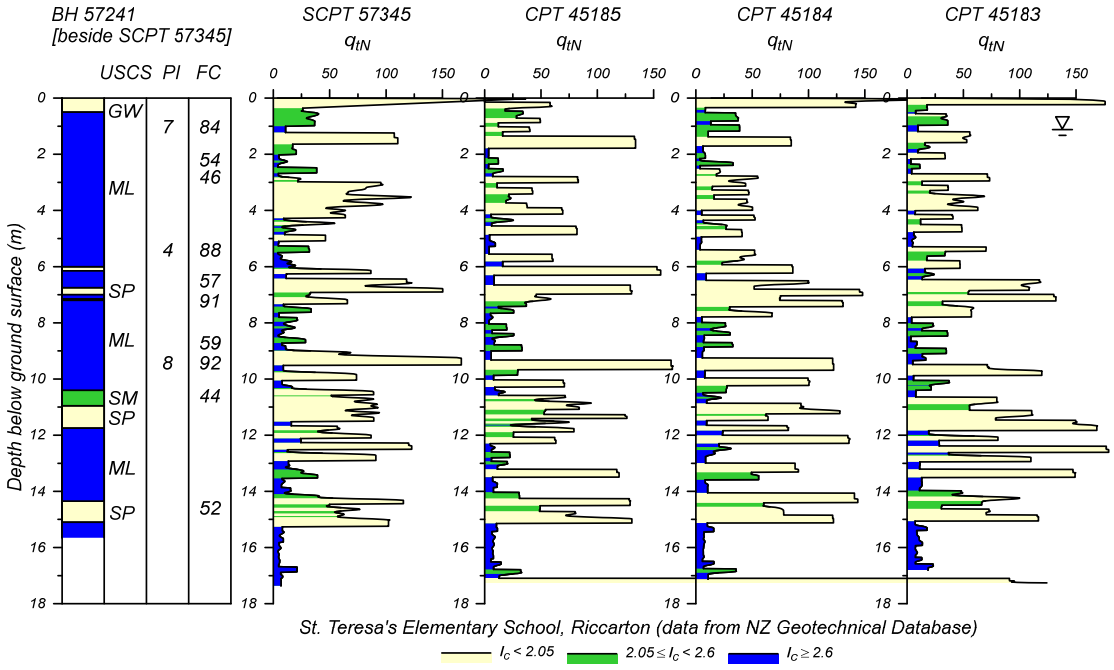

FIG. 6. Profile across St. Teresa's School site with the inverse filtered CPTs.

SITE AND LIQUEFACTION EVALUATIONS

LVI Procedures

Four liquefaction vulnerability indices were used in the present study: LDI, LPI, $S_{v\text{-}1D}$, and LSN. For all four LVIs, the potential for liquefaction triggering was evaluated using the simplified procedure (Seed and Idriss 1971) with the CPT-based liquefaction correlation by Boulanger and Idriss (2015). The four LVIs were also computed using the full depths of the CPT soundings.

The LDI, as named by Zhang et al. (2004), represents a potential maximum lateral ground surface displacement computed by integrating potential maximum shear strains (γ_{max}) over depth as,

$$LDI = \int_0^{z_{max}} \gamma_{max} dz \tag{1}$$

For the analyses presented herein, the potential maximum shear strains were computed using the approximation of Ishihara and Yoshimine's (1992) relationship described in Idriss and Boulanger (2008). For level ground conditions away from a free face, Tokimatsu and Asaka (1998) recommended that the dynamic strains (for computing dynamic ground lurch) are only about 10-20% of the above potential maximum shear strains. Thus, the dynamic ground lurch can be expected to be about 10-20% of the LDI value computed herein using potential maximum shear strains.

The LPI, developed by Iwasaki et al. (1978), is a depth-weighted function of the factor of safety against liquefaction triggering (FS) computed as,

$$LPI = \int_0^{z_{max}} \langle 1 - FS \rangle \langle 10m - 0.5z \rangle dz \tag{2}$$

where the Macaulay brackets $\langle\rangle$ restrict their arguments to be greater than or equal to zero.

The $S_{v\text{-}1D}$ represents a potential ground surface settlement computed by integrating post-liquefaction 1-D reconsolidation strains ($\varepsilon_{v\text{-}1D}$) over depth as,

$$S_{v-1D} = \int_0^{z_{max}} \varepsilon_{v-1D} dz \tag{3}$$

For the analyses presented herein, the potential reconsolidation strains were computed using the relationship by Zhang et al. (2002).

The LSN was introduced by van Ballegooy et al. (2014) based on experiences in Christchurch, and is a depth-weighted function of the post-liquefaction 1-D reconsolidation strains computed as,

$$LSN = 1000 \int_0^{z_{max}} \frac{\varepsilon_{v-1D}}{z} dz \tag{4}$$

where the potential reconsolidation strains are based on the relationship by Zhang et al. (2002).

The strengths and limitations of these LVIs for predicting the observed effects of liquefaction in Christchurch during the 2010-2011 Canterbury Earthquake Sequence, both at local and regional scales, have been studied extensively by others (e.g., van

Ballegooy et al. 2014, 2015, Maurer et al. 2014, 2015). These prior studies have generally concluded that liquefaction evaluations based on various LVIs and different liquefaction triggering correlations tend to over-predict liquefaction effects in the interbedded soil deposits encountered in various areas of Christchurch.

The following sections examine the application of these LVIs to the St. Teresa's School site. First, the site data are processed using the CPT-based triggering procedures by Boulanger and Idriss (2015) to calibrate the fines content parameter (C_{FC}) and develop distributions for the equivalent clean sand, overburden corrected, cone penetration resistances (q_{c1Ncs}). Second, results of the LVI evaluations are presented for several different sets of assumptions representing alternative practices and key sources of uncertainty in the LVI calculations. Lastly, more general limitations in the use of LVI procedures for predicting liquefaction effects are discussed.

Distributions of FC, I_c, and q_{c1Ncs}

The CPT and borehole data were processed using the CPT-based liquefaction triggering procedures by Boulanger and Idriss (2015) to calibrate the C_{FC} parameter for the interbedded stratum and develop distributions for q_{c1Ncs} with and without the site-specific C_{FC} calibration. The vertical and lateral variability of the interbedded stratum makes it extremely difficult to map individual FC measurements at the borehole 57241 location to corresponding I_c values at the nearby SCPT 57345 location. In such situations, it is often preferable to base the calibration of C_{FC} on mapping the median FC value in a given geologic stratum at a borehole location to the median I_c value in that same stratum at an adjacent CPT location. This approach is often a more stable basis for calibration of C_{FC} than a point-by-point comparison, and only requires that the distributions of FC and I_c are similar at the two adjacent locations.

Accordingly, the cumulative distributions of q_{cN} and I_c in the interbedded stratum at each of the four CPT locations were compared, as shown in Figure 7 for the measured CPT data, and found to be very similar at all four locations. The CPT data were subsequently binned into the sand-like and clay-like categories (using an I_c of 2.6 as the boundary) and the distributions for each category found to also be similar at the four locations. The cumulative distributions of I_c for SCPT 57345 (adjacent to borehole 57241) are shown in Figure 8 to illustrate both typical values and the effects of inverse filtering on these distributions; Figure 8a shows the distributions for all soils in the interbedded stratum, whereas Figure 8b shows separate distributions for the sand-like and clay-like categories. Inverse filtering reduced I_c values for the sand-like category (due to increases in q_{tN} values) and increased I_c values for the clay-like category (due to decreases in q_{tN} values). The median I_c value for the sand-like category without inverse filtering was 2.06 for SCPT 57345 or 2.08 if all four CPTs are considered. The median I_c value for the sand-like category with inverse filtering was reduced to 1.82 for SCPT 57345 or 1.86 if all four CPTs are considered. The median FC for the sand-like soils in boring 57241 is about 52%, from which the fines content parameter C_{FC} can be estimated as,

$$C_{FC} = \left(\frac{FC_{median} + 137}{80} \right) - I_{c,median} \quad (4)$$

This approach results in a C_{FC} value of 0.28 for use with the measured CPT data in the interbedded stratum and 0.50 for use with the inverse filtered CPT data. Note that the correlation by Boulanger and Idriss (2015) is based on measured CPT data (not inverse filtered data) and the corresponding standard deviation in C_{FC} is 0.29.

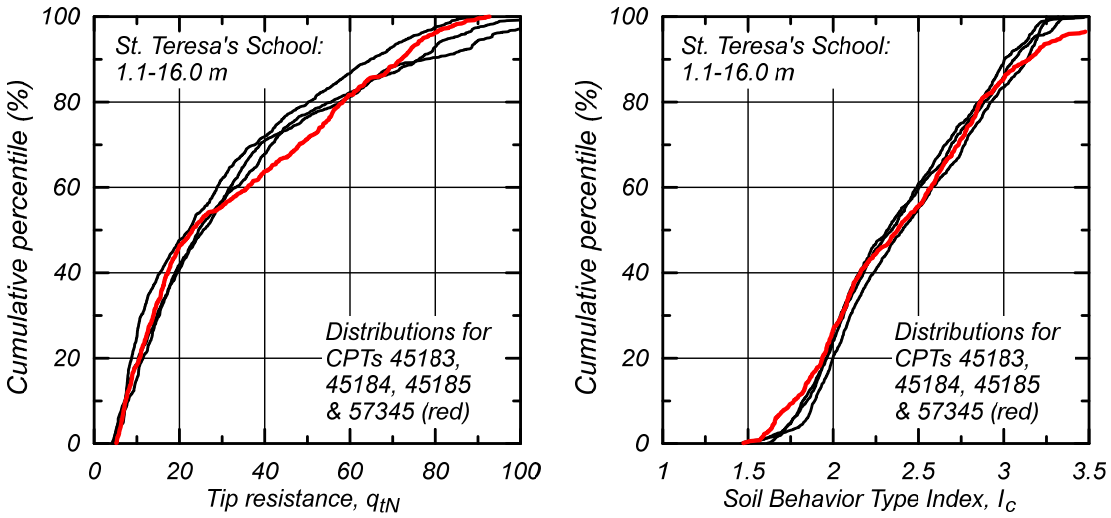

FIG. 7. Cumulative distributions of (a) q_{cN} and (b) I_c values for the interbedded stratum using the four measured CPT profiles.

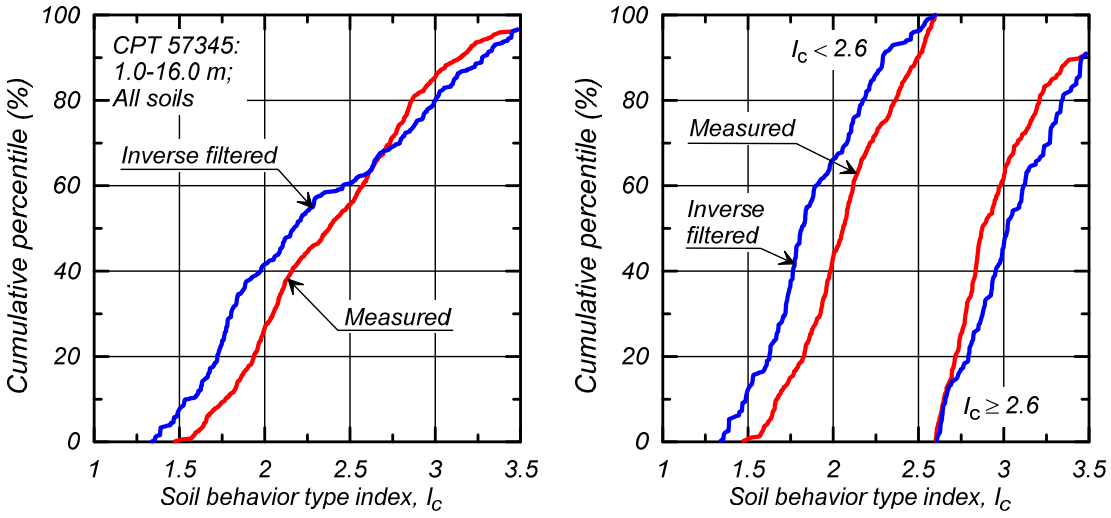

FIG. 8. Cumulative distributions of I_c for the interbedded soils between 1.1 and 16.0 m depth in SCPT 57345 with and without inverse filtering: (a) all soils, (b) soils with $I_c \geq 2.6$ or $I_c < 2.6$.

The above site-specific calibration for C_{FC} is compared in Figure 9 to the dataset and correlation for Christchurch soils compiled by Maurer et al. (2018). The correlation for Christchurch soils by Maurer et al. (2018) is approximately equal to the correlation by Boulanger and Idriss (2015) with $C_{FC} = 0.13$. The calibration of $C_{FC} = 0.28$ for the St. Teresa School site is below the general correlation, but within the scatter of the data. The calibration of $C_{FC} = 0.50$ for use with inverse filtered CPT data is toward the lower range of the scatter in the data, and this is partly attributed to the data in Figure 9 being based on measured CPT data and not inverse filtered data.

Cumulative distributions for FC in the sand-like soils of the interbedded stratum, as estimated using the data from SCPT 57345, are shown in Figure 10a. The median FC is estimated to be 28% using the measured CPT data with the default $C_{FC} = 0.0$ value, illustrating that the default correlation significantly underestimates the FC for these soils. The median FC is correctly estimated to be about 50% (matching the borehole data) using the measured and inverse filtered CPT data with their respective C_{FC} calibrations.

Cumulative distributions for q_{c1Ncs} in the sand-like soils of the interbedded stratum, as estimated using the data from SCPT 57345, are shown in Figure 10b. The median q_{c1Ncs} using the measured CPT data increases from about 122 to 142 when C_{FC} is increased from its default of 0.0 to the calibrated value of 0.28. The median q_{c1Ncs} further increases to about 186 using the inverse filtered CPT data with its calibrated C_{FC} value of 0.50. Similarly, the 33rd percentile values of q_{c1Ncs} were 102, 121 and 152 for these three cases, respectively. These shifts in the cumulative distributions are particularly important when selecting properties for use in nonlinear dynamic analyses, as prior studies have shown that 30th to 70th percentile values (or the 33rd percentile for deterministic practice) are generally appropriate as the equivalent representative values for use in numerical models with uniform properties (e.g., Montgomery and Boulanger 2016).

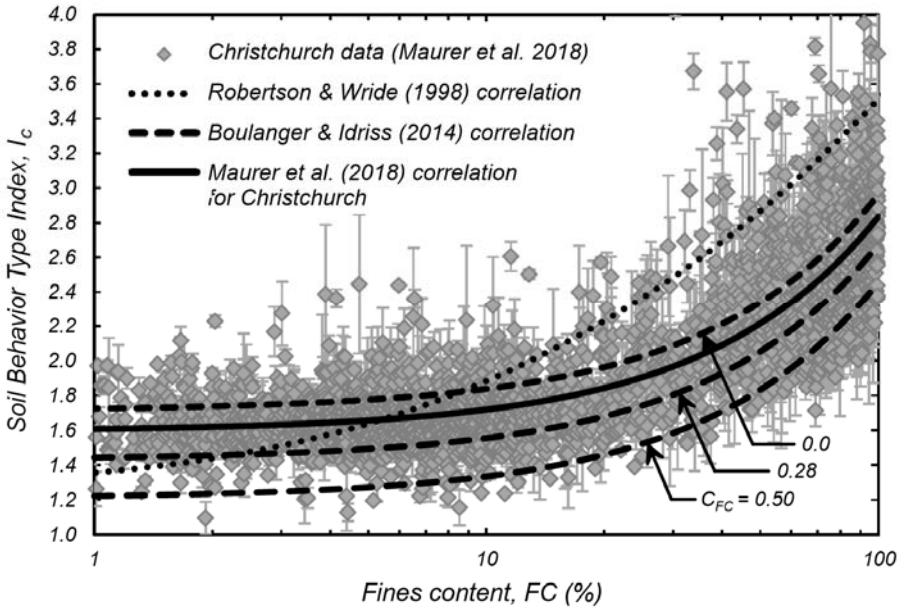

FIG. 9. Correlations between fines content and I_c compared to data from Christchurch (modified from Maurer et al. 2018)

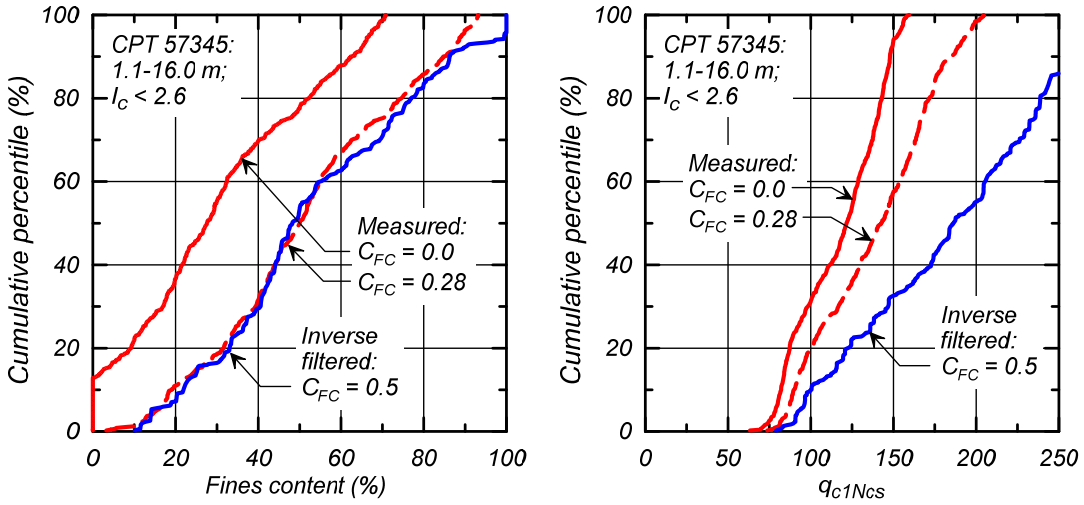

FIG. 10. Cumulative distributions for estimated fines content and q_{c1Ncs} based on measured CPT data, measured data with site-specific fines content calibration, and inverse filtered data with site-specific fines content calibration.

Results of LVI Evaluations

The four LVIs were computed for several cases involving some implementation alternatives, key sources of uncertainty, and a range of earthquake loadings. The LVIs computed using all four CPTs at the site gave similar results, and thus results are only presented for SCPT 57345 herein. In addition, the LVIs computed for the M_w=6.2 Christchurch earthquake (site PGA of 0.34 g) were greater than for the M_w=7.1 Darfield earthquake (site PGA of 0.22 g), so resolving the LVI results with the field observations for the Christchurch earthquake would resolve results for the Darfield earthquake as well. Accordingly, the trends and findings from the LVI evaluations are well represented by the subset of results shown in Figure 11. This figure shows the four LVIs versus PGA for an M_w = 6.2 earthquake using the data from SCPT 57345. Each plot shows results for five analysis cases, each of which is described below.

The first analysis case used the measured CPT data with the default C_{FC} = 0.0 often used in practice. All four LVIs begin to increase sharply once the PGA exceeds about 0.12 g, and all four LVIs reach values that would indicate major/severe liquefaction damage at a PGA of 0.34 g (the estimated PGA for Christchurch earthquake). For example, correlations between LPI and LSN values and observed damage levels have been developed by several investigators, from which the results in Table 1 are illustrative. The LPI and LSN values at a PGA of 0.34 g for the first analysis case in Figure 11 are consistent with severe liquefaction manifestation during the Christchurch earthquake based on the correlations in Table 1.

The second analysis case used the measured CPT data with the site-specific calibration of C_{FC} = 0.28. The inclusion of this site-specific fines content calibration reduced all four LVIs by about 20-35% across the range of PGAs examined (Figure 11). The LPI and LSN values for this analysis case, however, are still large enough that severe liquefaction manifestation would be expected during the Christchurch earthquake based on the correlations in Table 1.

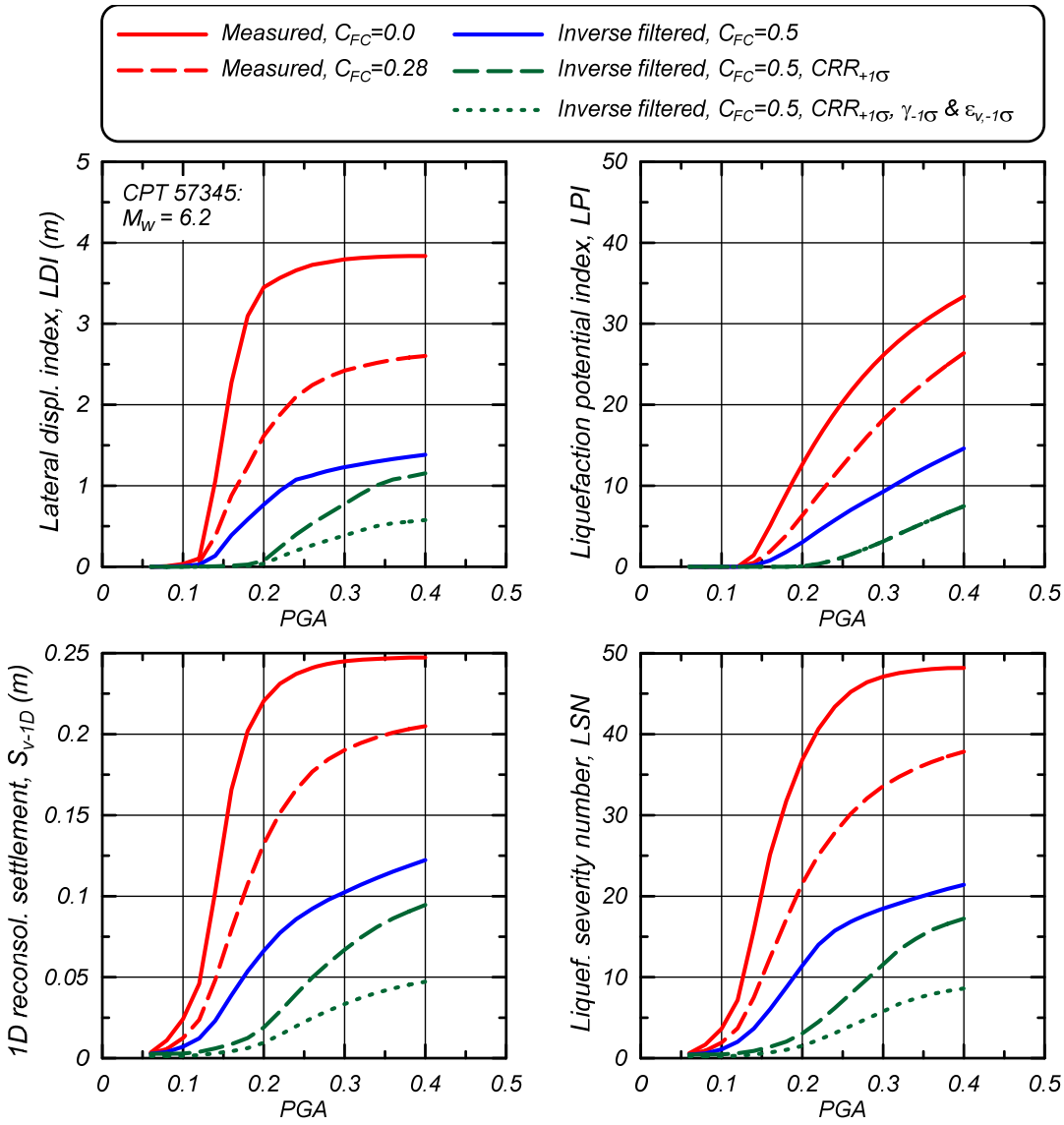

FIG. 11. Liquefaction vulnerability indices versus PGA computed for SCPT 57345 for an M_w=6.2 earthquake with different combinations of analysis assumptions.

Table 1. Threshold values for the LPI and LSN liquefaction vulnerability indices

Index	Reference	Severity of liquefaction manifestation		
		None to minor (non-damaging)	Moderate (damaging)	Major/severe
LPI	Wotherspoon et al. (2013)	< 5	5 - 15	> 15
	Maurer et al. (2014)	< 8	8 - 15	> 15
	McLaughlin (2017)	< 8	8 - 15	> 15
LSN	Wotherspoon et al. (2013)	< 20	20 - 50	> 50
	Tonkin+Taylor (2015, 2016)	< 16	16 - 30	> 30
	McLaughlin (2017)	< 16	16 - 26	> 26

The third analysis case used the inverse filtered CPT data with the site-specific calibration of C_{FC} = 0.50. The combination of inverse filtering with site-specific fines content calibration reduced all four LVIs by about 55-65% relative to the first analysis case. These two refinements to the LVI analysis are technically well justified and relatively easy to perform, and together they significantly reduce the discrepancy between predicted and observed damage levels. The LPI of about 12 and LSN of about 20 at a PGA of 0.34 g for this analysis case are now both consistent with moderate liquefaction manifestation during the Christchurch earthquake (Table 1).

The fourth analysis case examines the sensitivity of the LVIs to the uncertainty in the CPT-based triggering correlation. For deterministic applications, the CPT-based triggering correlation by Boulanger and Idriss (2015) is commonly used to obtain minus one standard deviation estimates of the CRR. For any given soil deposit, it is reasonable to expect that CRRs may be consistently bias high or low relative to the expected values. For example, the standard deviation is 0.20 (in natural logarithm units) for the Boulanger and Idriss correlation, such that the plus one standard deviation value for CRR is about 49% larger than the minus one standard deviation value (Figure 12). To illustrate the potential effect that this range of uncertainty in CRR values has on LVIs, the fourth analysis case uses the plus one standard deviation estimates for CRR in combination with the inverse filtering and site-specific fines content calibration (i.e., building on the third analysis case). The results in Figure 11 show that the four LVIs only begin to increase sharply after the PGA exceeds about 0.20 g, and reach values at a PGA of 0.34 g that are 67-83% smaller than obtained in the first analysis case. The LPI of about 5 and LSN of about 15 at a PGA of 0.34 g for this analysis case are now both near the thresholds between none-to-minor and moderate liquefaction manifestation based on Table 1.

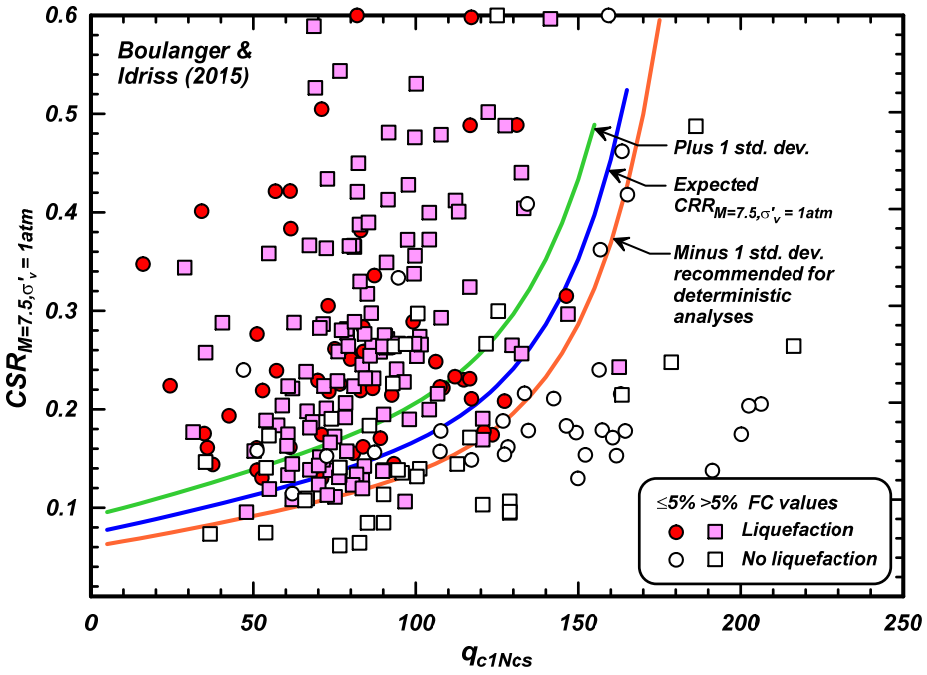

FIG. 12. CPT-based triggering correlation by Boulanger and Idriss (2015).

The fifth analysis case builds on the fourth case by adding the potential effects of uncertainty in the correlations used to estimate maximum potential shear strains and 1-D post-liquefaction reconsolidation strains. These correlations for shear and volumetric strains are primarily based on laboratory test data for clean sands and involve considerable uncertainty. For example, Cetin et al. (2009) developed a probabilistic correlation for reconsolidation strains, and obtained a standard deviation of 0.689 in natural logarithm units which corresponds to a factor of about 2.0 arithmetically. In addition, extending these correlations to silty sands and sandy silts is likely to involve even greater uncertainty. The shear and volumetric strains estimated by the correlations applicable for each LVI were reduced by a factor of 2.0 as an approximation of moving from expected values to minus one standard deviation values. In this regard, it seems reasonable to expect that soils that fall close to plus one standard deviation for CRR (e.g., due to age, over-consolidation, cementation, plasticity, or other factors), as considered in the fourth analysis case, would also tend to give lower than expected shear and volumetric strains. The results in Figure 11 show that the LDI, LSN, and $S_{v\text{-}1D}$ values are reduced by about 50% relative to the fourth analysis case while the LPI is unaffected, as expected. The LDI, LSN, and $S_{v\text{-}1D}$ at a PGA of 0.34 g are now only about 15% of the values obtained in the first analysis case. At a PGA of 0.34 g, the LPI of about 5 is at the threshold between none-to-minor and moderate liquefaction manifestation (Table 1), the LSN of about 8 is consistent with none-to-minor liquefaction manifestation (Table 1), the LDI of about 0.5 m would correspond to a dynamic ground lurch of only 50-100 mm based on the recommendations of Tokimatsu and Asaka (1998), and the computed $S_{v\text{-}1D}$ of about 40 mm is small enough that only minor surface manifestation would be expected for this level site with its lightly loaded structures.

The magnitudes of these LVIs for the fifth analysis case are at levels that would be consistent with the lack of observed liquefaction damages at this site in the 2010-2011 Canterbury Earthquake Sequence. These results suggest that the discrepancy between no observed liquefaction manifestations at the site and high LVIs computed using default practices (i.e., the first analysis case) can largely be resolved or understood by combining inverse filtering of the CPT data with site-specific calibration of the C_{FC} parameter, and then allowing for reasonable bounds on the accuracy of the correlations used to estimate cyclic strengths and resulting strains. The inverse filtering and C_{FC} calibration steps are technically justifiable in a forward analysis, whereas the results for the fourth and fifth analysis case demonstrate that the lack of observed liquefaction manifestations are within the expected accuracy limits of these LVI parameters once the other factors have been accounted for.

The effect of partial saturation in the upper portion of the soil profile was also examined. The cyclic resistance ratios for the sand-like soils in the upper 5.0 m were multiplied by a factor of 1.15 based on the measured V_p of 800-1,100 m/s in these soil types and the relationships in Ishihara and Tsukamoto (2004). Combining this effect with the fifth analysis case reduced the four LVIs by relatively small amounts for this case, in part because the factors of safety against liquefaction triggering at shallow depths were already relatively large. Combining this effect with the first analysis case caused a greater percentage reduction in the LVIs, but it was still of secondary importance to the other factors for this site.

Other Potential Sources of Bias in LVI-based Evaluations

Other potential sources of conservative bias in LVI-based liquefaction evaluations for interbedded soil deposits stem from basic limitations in the analysis approach. LVI procedures rely on the Seed-Idriss Simplified Procedure for estimating the cyclic stresses imposed at different depths in the soil profile, which inherently neglects key aspects of dynamic response and excess pore pressure diffusion, which can have a strong effect on ground deformations. For example, Cubrinovski et al. (2017) performed nonlinear dynamic analyses for layered soil profiles representative of conditions encountered in different areas of Christchurch (including the St. Teresa School site), and showed that the system response can: (1) intensify liquefaction damages for sites with relatively thick, vertically continuous, liquefiable zones in the upper 10 m, where the upward flow of pore water can intensify strength loss and deformations at shallow depths, or (2) mitigate liquefaction manifestation in interbedded sites where liquefaction in a deeper layer may reduce seismic demands on overlying layers and the lower permeability layers reduce the rate of upward seepage and its associated damaging effects. The manifestation of liquefaction effects at an interbedded site can also be reduced by the presence of a sufficiently thick, competent crust layer (e.g., Ishihara 1985), or by the composite resistance that interbedded liquefied and nonliquefied soils may provide against ground deformations (e.g., Munter et al. 2017).

The expected distribution of liquefaction versus depth at the St. Teresa School site is illustrated in Figure 13, showing profiles of $S_{v\text{-}1D}$ during the Darfield earthquake (Figure 13b) and Christchurch earthquake (Figure 13c) for the various analysis cases presented previously. Liquefaction and associated strains are expected to occur in multiple thin intervals of sand-like soils that are relatively uniformly distributed throughout the interbedded stratum (i.e., depths of 1.1 to 15 m). The soil profile indicates relatively continuous horizontal layering (Figure 2), such that liquefaction of layers at larger depths (e.g., depths greater than 6 to 10 m) would be expected to cause relatively uniform ground surface settlements (i.e., limited differential settlement) that may be difficult to observe. In addition, liquefaction along any of the deeper sand-like layers would be expected to reduce demands on the shallower layers, as shown by Cubrinovski et al. (2017), which would contribute to a thicker, stronger surface crust layer. The buildings at the site are also relatively light, which reduces the demands imposed on the surface crust layer. Overall, it is reasonable to expect the system response for this interbedded soil profile to have helped mitigate against liquefaction manifestations, which also could explain possible discrepancies between the LVIs computed by the third or fourth analysis case and the lack of observed damages at this site during these earthquakes.

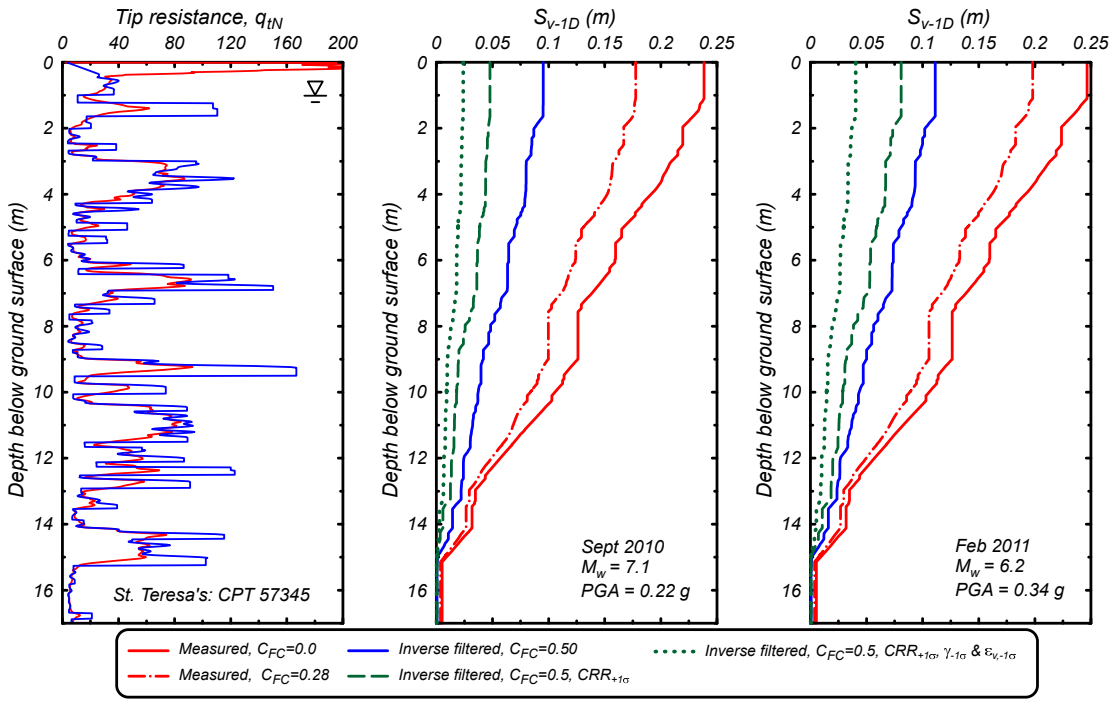

FIG. 13. $S_{v\text{-}1D}$ profiles for the September 2010 Darfield and February 2011 Christchurch earthquakes for SCPT 57345 with different combinations of analysis assumptions.

CONCLUSIONS

A liquefaction evaluation using four different liquefaction vulnerability indices (LDI, LPI, $S_{v\text{-}1D}$, LSN) was performed for St. Teresa's School site in Christchurch, New Zealand to evaluate why LVI computations using common practices overestimated the potential for liquefaction damages at this interbedded soil site during the 2010-2011 Canterbury Earthquake Sequence. The site is underlain by an approximately 16-m-thick stratum of interbedded silt, sandy silt, silty sand and sand. There was no reported liquefaction damage following either the 2010 M_w=7.1 Darfield earthquake or the 2011 M_w=6.2 Christchurch earthquake despite estimated peak ground accelerations of 0.22 g and 0.34 g in these two events, respectively.

All four LVIs were reduced by about 55-65% relative to default practices by incorporating two additional steps in the analysis: (1) applying an inverse filtering procedure to the CPT data to approximately correct for thin-layer and transition zone effects, and (2) performing a site-specific calibration for the fines content parameter used in the CPT-based liquefaction triggering correlation. The inverse filtering procedure was recently developed by Boulanger and DeJong (2018), and thus this case study provides an assessment of its application to a liquefaction evaluation.

The LVI values obtained using the above additional steps, combined with allowances for uncertainty in the correlations used to estimate cyclic strengths and resulting strains, can reach levels that are consistent with the lack of observed liquefaction manifestations. These results illustrate that the field observations are

within the expected accuracy limits of these LVI parameters once the other factors have been accounted for. These results also illustrate the need for additional work examining potential biases in current liquefaction correlations when applied to the types of silty soils encountered at this site.

The system response for this interbedded soil site can be expected to have further mitigated liquefaction manifestation as shown by the numerical analyses of interbedded profiles performed by Cubrinovski et al. (2017): (1) liquefaction in a deeper layer may reduce seismic demands on overlying layers and (2) the lower permeability layers will reduce the rate of upward seepage and thus reduce the strength loss and deformation it can cause at shallow depths.

In summary, the tendency for LVIs computed using default practices to over-predict liquefaction effects at interbedded sites during the 2010-2011 Canterbury Earthquake Sequence, such as at the St. Teresa School site, is most likely due to the cumulative effects of various limitations in our site characterization tools, correlations, and analysis procedures. Eliminating the tendency for LVI-based liquefaction evaluations to overestimate liquefaction damages will require efforts to address limitations in each of these areas.

ACKNOWLEDGMENTS

The authors appreciate the financial support of the National Science Foundation (award CMMI-1635398), California Department of Water Resources (contract 4600009751), and the Pacific Earthquake Engineering Research Center for different aspects of the work presented herein. Any opinions, findings, conclusions, or recommendations expressed herein are those of the authors and do not necessarily represent the views of these organizations. The site characterization data was sourced from the New Zealand Geotechnical Database. The analyses of St. Teresa's School site have benefited from various discussions and collaborations with Sjoerd van Ballegooy, Jonathan Bray, Misko Cubrinovski, Kaleigh McLaughlin, Ken Stokoe, and Liam Wotherspoon. The authors are grateful for the above support and interactions.

REFERENCES

Ahmadi, M. M. and Robertson, P. K. (2005). "Thin-layer effects on the CPT q_c measurement." Canadian Geotechnical Journal, 42(5), 1302-1317.

Beyzaei, C. Z., Bray, J. D., Cubrinovski, M., Riemer, M., and Stringer, M. E. (2018). "Laboratory-based characterization of shallow silty soils in southwest Christchurch." Soil Dynamics and Earthquake Engineering, 110: 93-109.

Boulanger, R. W., and DeJong, J. T. (2018). "Inverse filtering procedure to correct cone penetration data for thin-layer and transition effects." Proceedings, CPT18 – 4th International Symposium on Cone Penetration Testing, Delft, The Netherlands.

Boulanger, R. W. & Idriss, I. M. (2015). "CPT-based liquefaction triggering procedure." J. of Geotechnical and Geoenvironmental Engineering, ASCE, 142(2): 04015065, 10.1061/(ASCE)GT.1943-5606.0001388.

Boulanger, R. W., Moug, D. M., Munter, S. K., Price, A. B., and DeJong, J. T.

(2016). "Evaluating liquefaction and lateral spreading in interbedded sand, silt, and clay deposits using the cone penetrometer." 5th International Symposium on Geotechnical and Geophysical Site Characterisation, B. M. Lehane, H. Acosta-Martinez, and R. Kelly, eds., Australian Geomechanics Society, Sydney, Australia, ISBN 978-0-9946261-2-7.

Bradley, B. A. (2014). "Site-specific and spatially-distributed ground motion intensity estimation in the 2010-2011 Canterbury earthquakes." Soil Dynamics and Earthquake Engineering, 61-62: 83-91.

Cetin, K. O., Bilge, H. T., Wu, J., Kammerer, A. M., and Seed, R. B. (2009). "Probabilistic model for the assessment of cyclically induced reconsolidation (volumetric) settlement." J. of Geotechnical and Geoenvironmental Engineering, ASCE, 135(3): 387-398.

Cox, B. R., McLaughlin, K. A., van Ballegooy, S., Cubrinovski, M., Boulanger, R. W., and Wotherspoon, L. 2017. In-situ investigation of false-positive liquefaction sites in Christchurch, New Zealand: St. Teresa's School case history. Proc., Performance-based Design in Earthquake Geotechnical Engineering, PBD-III Vancouver, M. Taiebat et al., eds., ISSMGE Technical Committee TC203, paper 265.

Cubrinovski, M., Rhodes, A., Ntritsos, N., and van Ballegooy, S. (2017). "System response of liquefiable soils." Proc., Performance-based Design in Earthquake Geotechnical Engineering, PBD-III Vancouver, M. Taiebat et al., eds., ISSMGE Technical Committee TC203, paper 540.

Green, R.A., Cubrinovski, M., Cox, B., Wood, C., Wotherspoon, L., Bradley, B. and Maurer, B. (2014). "Select Liquefaction Case Histories from the 2010–2011 Canterbury Earthquake Sequence." Earthquake Spectra, 30(1): 131-153.

Idriss, I. M. and Boulanger, R. W. (2008). Soil liquefaction during earthquakes. Monograph MNO-12, Earthquake Engineering Research Institute, Oakland, CA, 261 pp.

Ishihara K. (1985). "Stability of natural deposits during earthquakes." Proceedings, 11th International Conference on Soil Mechanics and Foundation Engineering, San Francisco. Vol. 1, p. 321-376.

Ishihara, K. and Tsukamoto, Y. (2004). "Cyclic strength of imperfectly saturated sands and analysis of liquefaction." Proceedings of the Japan Academy, 80B(8): 372-391.

Ishihara, K. and Yoshimine, M. (1992). "Evaluation of settlements in sand deposits following liquefaction during earthquakes." Soils and Foundations, Japanese Geotechnical Society, 32(1): 173-188.

Iwasaki, T., Tatsuoka, F., Tokida, K., and Yasuda, S. (1978). "A practical method for assessing soil liquefaction potential based on case studies at various sites in Japan." Proceedings of the 2nd International Conference on Microzonation, Nov 26-Dec 1, San Francisco, CA, USA.

Khosravi, M., Boulanger, R. W., Khosravi, A., DeJong, J. T., Hajialilue-Bonab, M., and Wilson, D. W. (2018). "Centrifuge modeling of cone penetration testing in layered soil." Proc., Geotechnical Earthquake Engineering and Soil Dynamics V, Austin, TX, ASCE.

Maurer, B.W., Green, R.A., Cubrinovski, M. and Bradley, B.A. (2014). "Evaluation

of the Liquefaction Potential Index for Assessing Liquefaction Hazard in Christchurch, New Zealand." J. Geotechnical and Geoenvironmental Engineering, ASCE, 140(7): 04014032, 10.1061/(ASCE)GT.1943-5606.0001117.
Maurer, B.W., Green, R.A., and Taylor, O.S. (2015). "Moving towards an improved index for assessing liquefaction hazard: Lessons from historical data." Soils and Foundations, JGS, 55(4): 778-787.
Maurer, B. W., Green, R. A., van Ballegooy, S., and Wotherspoon, L. (2018). "Development of region-specific soil behavior type index correlations for evaluating liquefaction hazard in Christchurch, New Zealand." Soil Dynamics and Earthquake Engineering, in-press.
McLaughlin, K. (2017). Investigation of false-positive liquefaction case history sites in Christchurch, New Zealand. M.S. Thesis. The University of Texas at Austin.
Mo, P.-Q., Marshall, A. M., and Yu, H.-S. (2017). "Interpretation of cone penetration test data in layered soils using cavity expansion analysis." J. Geotechnical and Geoenvironmental Eng., 143(1), 10.1061/(ASCE)GT.1943-5606.0001577.
Montgomery, J., and Boulanger, R. W. (2016). "Effects of spatial variability on liquefaction-induced settlement and lateral spreading." Journal of Geotechnical and Geoenvironmental Engineering, ASCE, 2017, 143(1), 04016086, 10.1061/(ASCE)GT.1943-5606.0001584.
Munter, S. K., Boulanger, R. W., Krage, C. P., and DeJong, J. T. (2017). "Evaluation of liquefaction-induced lateral spreading procedures for interbedded deposits: Cark Canal in the 1999 M7.5 Kocaeli earthquake." Geotechnical Frontiers 2017, Seismic Performance and Liquefaction, Geotechnical Special Publication No. 281, T. L. Brandon and R. J. Valentine, eds., 254-266.
New Zealand Geotechnical Database (2018). Retrieved March 10, 2018 from https://www.nzgd.org.nz
Robertson, P. K. (1990). "Soil classification using the cone penetration test." Canadian Geotechnical Journal, 27(1), 151–58.
Robertson, P. K. (2009). "Interpretation of cone penetration tests – a unified approach." Canadian Geotechnical Journal, 46, 1337-1355.
Seed, H. B., and Idriss, I. M. (1971). "Simplified procedure for evaluating soil liquefaction potential." J. Soil Mechanics and Foundations Div., ASCE 97(SM9), 1249–273.
Stringer, M., Beyzaei, C., Cubrinovski, M., Bray, J. D., Riemer, M., Jacka, M. and Wentz, F. (2015). "Liquefaction characteristics of Christchurch silty soils: Gainsborough Reserve." 6th International Conference on Earthquake Geotechnical Engineering, November 1-4, Christchurch, New Zealand.
Tokimatsu, K., and Asaka, Y. (1998). "Effects of liquefaction-induced ground displacements on pile performance in the 1995 Hyogoken-Nambu earthquake." Special Issue of Soils and Foundations, Japanese Geotechnical Society, 163-177.
Tonkin & Taylor Ltd. (2015). Canterbury Earthquake Sequence: Increased Liquefaction Vulnerability Assessment Methodology. Chapman Tripp acting on behalf of the Earthquake Commission (EQC), Tonkin & Taylor ref. 52010.140.v1.0.
Tonkin & Taylor Ltd. (2016). Practical implications of increased liquefaction vulnerability. Chapman Tripp acting on behalf of the Earthquake Commission

(EQC), Tonkin & Taylor ref. 52010.140.v2.0 0032-4-R-CPE-2016.
van Ballegooy, S., Malan, P., Lacrosse, V., Jacka, M. E., Cubrinovski, M., Bray, J. D., O'Rourke, T. D. O., Crawford, S. A. and Cowan, H. (2014). "Assessment of liquefaction-induced land damage for residential Christchurch." Earthquake Spectra, EERI, 30(1), 31-55.
van Ballegooy, S., Wentz, F. & Boulanger, R. W. (2015). "Evaluation of CPT-based liquefaction procedures at regional scale." Soil Dynamics and Earthquake Engineering, 10.1016/j.soildyn.2015.09.016.
Wotherspoon, L., Orense, R., Green, R., Bradley, B., Cox, B., & Wood, C. (2013). "Analysis of liquefaction characteristics at Christchurch strong motion stations." Proceedings, New Zealand – Japan Workshop on Soil Liquefaction during Recent Large-Scale Earthquakes, Auckland, New Zealand, December.
Xu, X. T., and Lehane, B. M. (2008). "Pile and penetrometer end bearing resistance in two-layered soil profiles." Géotechnique, 58(3), 187–197.
Zhang, G., Robertson, P.K. and Brachman, R.W.I. (2002). "Estimating liquefaction-induced ground settlements from CPT for level ground." Canadian Geotechnical Journal, 39: 1168-1180.